

We are IntechOpen, the world's leading publisher of Open Access books Built by scientists, for scientists

6,900

Open access books available

186,000

International authors and editors

200M

Downloads

Our authors are among the

154

Countries delivered to

TOP 1%

most cited scientists

12.2%

Contributors from top 500 universities



WEB OF SCIENCE™

Selection of our books indexed in the Book Citation Index
in Web of Science™ Core Collection (BKCI)

Interested in publishing with us?
Contact book.department@intechopen.com

Numbers displayed above are based on latest data collected.
For more information visit www.intechopen.com



Synthesis, Self-assembly and Optoelectronic Properties of Monodisperse ZnO Quantum Dots

Ting Mei^{1,2} and Yong Hu³

¹*Institute of Optoelectronic Materials and Technology, South China Normal University, Guangzhou 510631,*

²*School of Electrical and Electronic Engineering, Nanyang Technological University, 639798,*

³*Institute of Physical Chemistry, Zhejiang Normal University, Jinhua, 321004,*

^{1,3}*China*

²*Singapore*

1. Introduction

Quantum dot (QD), also called artificial atom, is a semiconductor nanocrystal with the size on the order of a few nanometers. By modifying its composition, size and shape, its density of electronic states can be engineered and thus many physical properties can be widely and easily adjusted. Strong quantum confinement of electronic carriers at nanometer scale makes band-gap and luminescence energies size and shape dependent. These dots have now been widely employed as targeted fluorescent labels for biomedical applications.

Zinc oxide (ZnO) is a wide-band-gap semiconductor that presents interesting luminescent properties, which are seen in the recent demonstration of ultraviolet lasing from nanowires. These properties have stimulated the search for new synthetic methodologies for well-controlled ZnO nanostructures. However, many applications require the organization of nanoparticles into two- or three-dimensional (2D or 3D) superlattices. This very efficient organization was obtained by physical methods, whereas chemical approaches toward such organizations would also be of interest since they are easy to perform and allow a facile scale-up procedure.

For the interest of size dependent physical properties, intensive research has been focused on fabricating ZnO QDs with ultra small size that gives strong quantum confinement. By far, various kinds of synthetic approaches have been realized in fabricating such small ZnO QDs, which can be roughly divided into two categories, chemical and physical. Chemical methods involves sol-gel method, hydrothermal growth, thermal decomposition, electrochemical method, while physical methods involves pulsed laser ablation (PLA or PLD), metalorganic chemical vapor deposition (MOCVD), radio frequency (RF) sputtering, flame spray pyrolysis (FSP) method, vapor phase transport (VPT) deposition, etc.. Chemical process takes advantage of the very exothermic reaction of the organometallic precursor bis(cyclohexyl) zinc with water to produce crystalline zinc oxide on one hand, and on the other hand the kinetic control of the decomposition by using long-alkyl-chain amine ligands. However, if the use of amine ligands allows access to ZnO nanoparticles with low size dispersity, these particles are not monodispersed, and consequently no 2D organization

was observed. For metal-oxide nanoparticles, a few 2D organizations resulting from particle self-assembly on a surface have been described. ZnO nanoparticles are produced by evaporating the solvent of the reaction solution, a method used in molecular chemistry to form monocrystals. In addition, the synthesis of ZnO nanoparticles is stabilized by combination of amine and acid ligands and their spontaneous organization into 2D ordered superlattices from colloidal solutions.

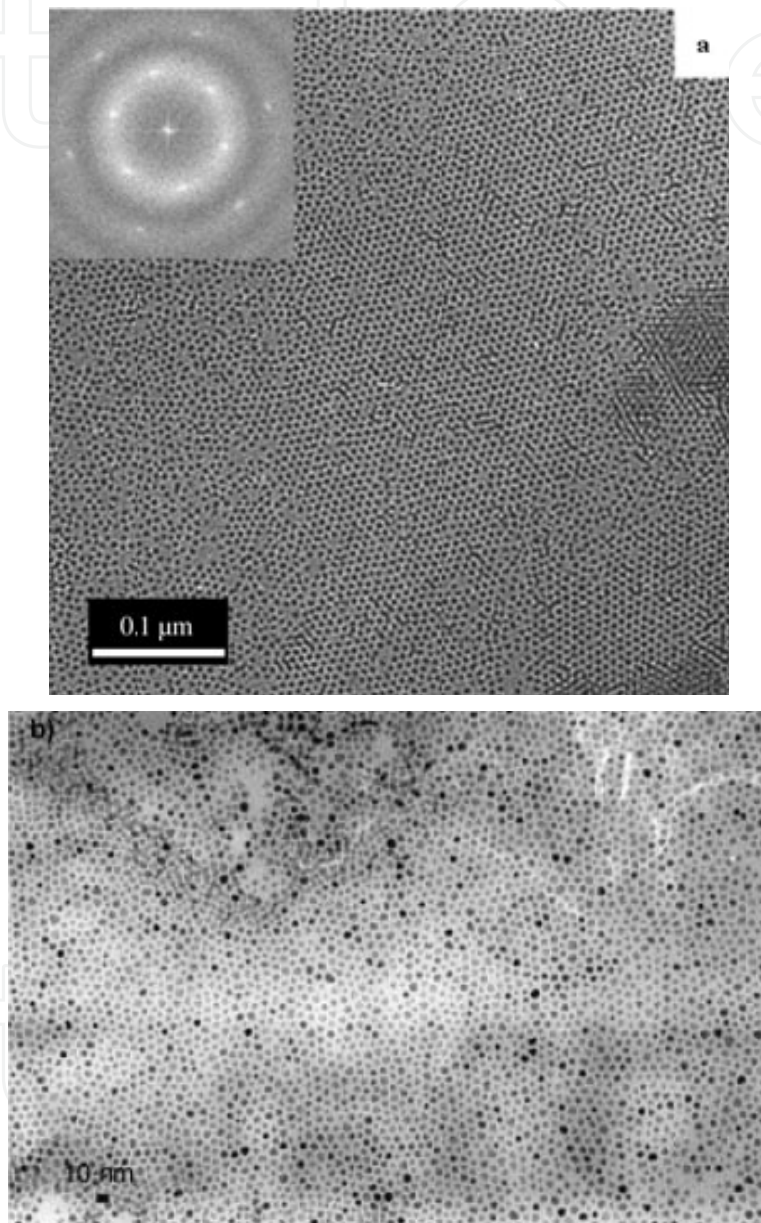


Fig. 1. a) 2D assembly of ZnO nanoparticles. b) ZnO nanocrystals following a slow oxidation/evaporation process in THF (two weeks)

If the synthesis is carried out in similar conditions but in the absence of solvent, a liquid fraction is formed even if the reagents are initially solids. For whatever the proportions of the components, the reaction yields isotropic nanoparticles, in contrast to the long nanorods obtained when only longalkylchain amines are present. This probably results in modification of the self-organization of the ligands. The size of the particles obtained under

these conditions is independent of the reaction conditions and similar to those resulting from the reaction in THF, but with greater dispersity. This therefore explains why 2D organizations have been previously obtained only with nanoparticles synthesized in THF (see Figure i).

The fundamental study of electronic properties of ZnO QDs is crucial for developing their future applications in nanoelectronics. Electronic transport measurements have been performed on individual ZnO nanowires and nanorods. Recently, the electroluminescence from 2D ZnO nanocrystals have been reported. Intrinsic optical properties of ZnO QDs are being intensively studied for implementing photonic devices. Photoluminescence (PL) spectra of ZnO QDs have also been extensively reported.

In this chapter, we investigate the synthesis and self-assembly of ZnO QDs and attempt to correlate with the optoelectronic properties. The results provide an insight on optoelectronic applications of ZnO QDs.

2. Synthesis of ZnO QDs

In past decades, zero-dimensional (0D) semiconductor nanocrystals, mainly known as QDs or quantum particles, have attracted much attention due to their potential for investigating the dependence of electronic transport or photoelectron emission properties on dimensionality and size reduction (so-called quantum confinement) [1, 2]. Applications of QDs on biology, photovoltaic devices, solar cells, sensors and QD-LEDs also have gained great interest in their relative research fields [3-7]. Much effort has been devoted to fabricating and developing compound semiconductor QDs, such as CdSe, CdTe, GaAs, InAs, InP, ZnS and ZnO [8-14]. A number of synthetic approaches have been used to fabricate those QDs, such as sol-gel [15], hydrothermal growth [16], thermal decomposition [17], pulsed laser ablation [18], flame spray pyrolysis [19], etc. [20, 21].

Zinc oxide (ZnO) is a direct band-gap ($E_g = 3.37\text{eV}$) semiconductor with an exciton binding energy as large as 60 meV at room temperature. The properties of near UV emission and transparent conduction can be exploited in optoelectronic devices such as solar cells, ultraviolet detectors, blue LEDs and LDs [22, 23]. ZnO is a bio-safe material that can be safely used in biological application such as bio-luminescence and bio-sensors [24, 25]. To make use of the size-dependent physical properties, intensive research has been focusing on fabrication of ZnO QDs with ultra small size (<10nm) for better quantum confinement. By far, various kinds of synthetic approaches have been realized in fabricating such small ZnO QDs, which can be roughly divided into chemical methods and physical methods. Chemical methods involves sol-gel method [26-40], hydrothermal growth [41-44], thermal decomposition [45-50], electrochemical method [51-54], while physical methods involves PLA or PLD [55-59], MOCVD [60-63], sputtering [64-66], FSP method [67-70] and VPT deposition [71, 72]. At present, all the methods can be divided into two parts as follow:

3. Chemical methods on synthesis of ZnO QDs

1. Sol-gel method

Sol-gel method, one of the widely used wet chemical methods in synthesizing various nanomaterials [15, 73-75], has been used for fabrication of ZnO QDs [26-40]. Among a number of reports on fabrication of ZnO QDs over the past decades, sol-gel method was the mostly used one due to its simplicity and cheapness. In this method, neither expensive equipments nor harsh conditions are needed. Tokumoto et al and many other research

groups have reported synthesis ZnO QDs at low temperature, i.e., less than 80°C [27-32]. Meulenkamp has reported a synthetic process with the highest temperature at only room temperature to make as-prepared ZnO QDs at a size of 3-6nm [29].

In typical preparation of ZnO QDs, zinc acetate dehydrate ($\text{Zn}(\text{CH}_3\text{COO})_2 \cdot 2\text{H}_2\text{O}$) or purity zinc acetate ($\text{Zn}(\text{CH}_3\text{COO})_2$) was mostly chosen as Zn precursor, while it is much more flexible to choose other reagents as oxygen source, such as lithium hydroxide (LiOH) [4-8], sodium hydroxide (NaOH) [9-13], Monoethanolamine (MEA) [14,15], Diethylene Glycol (99.5% DEG, ethylenediamine-tetra-acetic acid (EDTA)) [16,17], Triethanolamine (TEA) [18] and water [19,20]. Various alcohols like ethanol [4-8,12,14,], propanol [9-13,19,20] were used as solvents. The procedures of fabricating ZnO QDs are quite simple. Zn precursor and oxygen source were dissolved into alcoholic solvent respectively at a certain temperature with vigorous stirring before cooling down to or below room temperature. Then, these two alcoholic solutions were mixed by adding one solution into the other drop by drop with vigorous stirring at a certain temperature near freezing point. After that, aging or heating was performed to obtain solid ZnO QDs from ZnO sol-gels. Figure 1 shows some TEM images of ZnO QDs prepared by Yadav et al [28]. The size of as-prepared ZnO QDs is arranged from 1nm to 5nm.

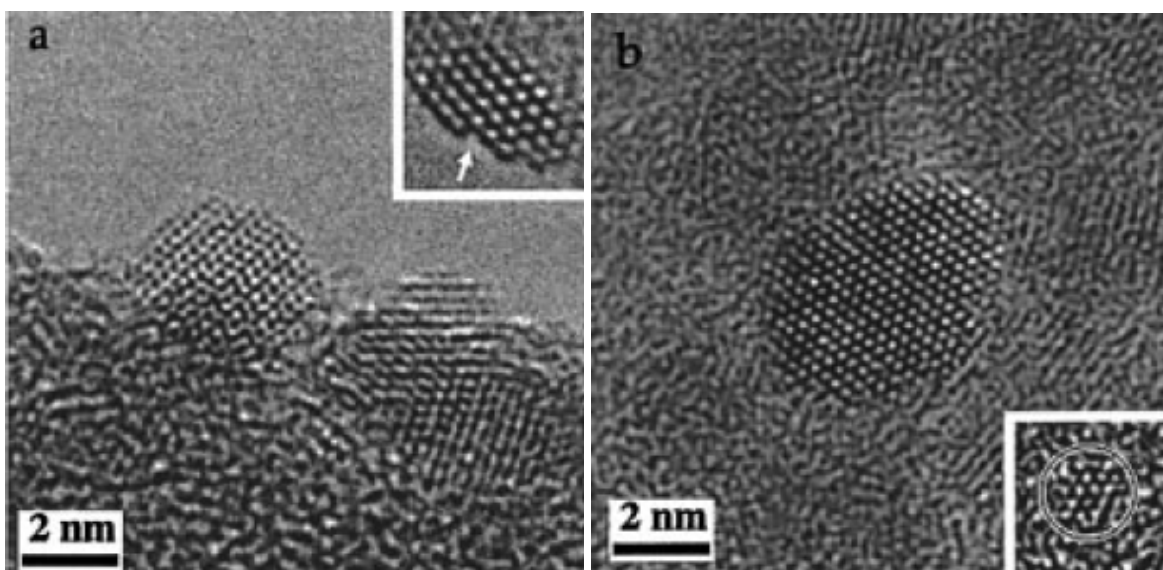


Fig. 1. ZnO QDs synthesized from zinc acetate dehydrate and sodium hydroxide (a) ZnO QDs about 3.7nm in diameter and approximately spherical in shape. The QD shown in the inset demonstrates strong faceting with a surface step consisting of a single atomic layer. (b) A single-crystal ZnO QD that exhibits evidence of faceting and the inset shows a ZnO QD approximately 1.5nm in diameter. (Courtesy of H. K. Yadav et al., [28])

Some detailed studies showed that the growth kinetics of ZnO QDs from colloidal suspensions follows the Lifshitz-Slyozov-Wagner theory for Ostwald ripening and the radius of as-prepared QDs is directly proportional to growth time [31, 32]. It was also shown that the average size of QDs can be tailored by the concentration of zinc precursor [37].

2. Hydrothermal growth

Solvent-thermal growth method is one of the widely used methods in liquid phase. As reactions were most probably occurred in aqueous solution, solvent-thermal growth method was well known as hydrothermal growth method. It is a simple, reliable and effective

method in synthesizing nanomaterials with different shapes under low supersaturation and mild conditions [16, 76-78]. ZnO QDs [41-43] as well as other nanostructures, such as nanowires, nanorods, nanotubes and other special shapes [79-83], has been fabricated using hydrothermal growth method. Hu et al [41] has reported fabrication of ZnO QDs with an average size of 3.5nm and good monodispersity (figure 2).

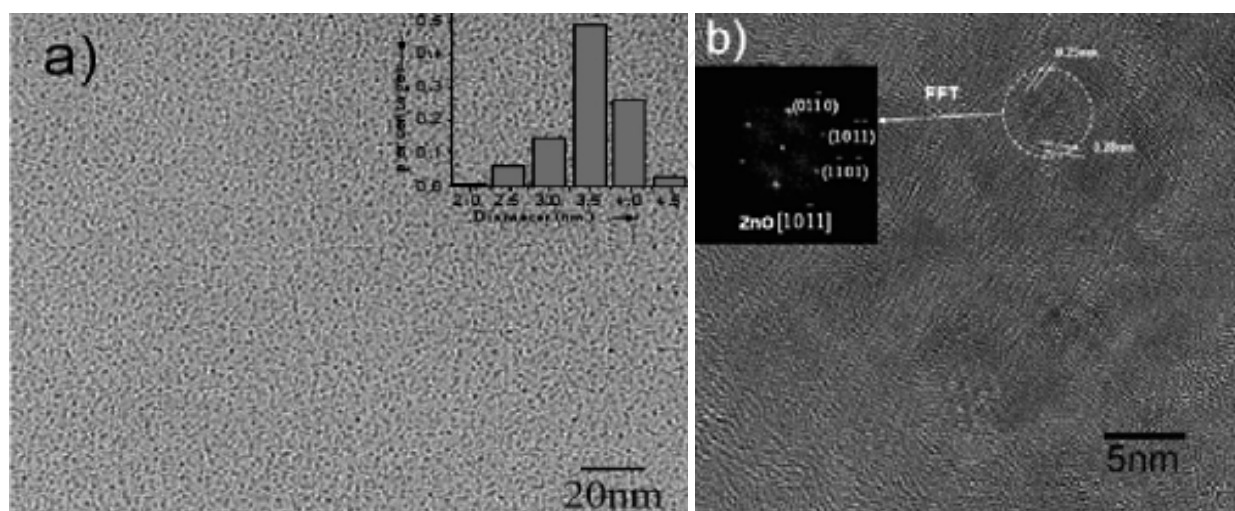


Fig. 2. Characterization of monodisperse ZnO QDs prepared by hydrothermal growth method. (a) Bright field TEM image and histogram of the size distribution (inset). (b) HRTEM image with fast Fourier transform (FFT) of the ZnO QDs. [41]

In a typical synthesis procedure, both inorganic zinc salts, such as ZnCl_2 [41, 42], ZnSO_4 [43], and organic zinc salts like $\text{Zn}(\text{CH}_3\text{COO})_2 \cdot 2\text{H}_2\text{O}$ [44] were used as zinc source, while NaOH [41, 42, 44] and KOH [43] were used as oxygen source. Both alcohol (ethanol [41, 42] and methanol [44]) and deionized water [41-43] could be used as solvent. Zinc salts were firstly dissolved in solvent with ultrasonic vibration and the same treatment was done for the alkali metal hydroxides at room temperature. After mixing those two prepared solutions by stirring, the final solution was transferred to a sealed autoclave and heated at relatively high temperature for hours. After centrifugation of the solution, ZnO QDs was obtained by washing with deionized water and alcohol as well as drying in the air.

Different from sol-gel method, sealed autoclaves were used to get high pressure and higher temperature was needed in hydrothermal growth process. The introduction of high pressure and high temperature accelerated the processes of synthesis. Therefore, less time was needed compare to the long time procedure of sol-gel process.

3. Thermal decomposition

Thermal decomposition method, based on decomposition of metal salts or metal oxides through heating, is theoretically and experimentally simple. To the best of our knowledge, there have been many metal oxides nanoparticles, such as Fe_2O_3 , NiO, Co_3O_4 and ZnO [84-87], synthesized via thermal decomposition method. However, there are not many reports on synthesizing ZnO quantum dots with ultra small size [45-50]. Fabrication of ZnO QDs with an average size of 1-10nm by decomposing zinc salts have reported by Cozzoli et al (Figure 3) [47].

The thermal decomposition of ZnO precursors could be taken place either in liquid or air environments. As for synthesis taken place in liquid environment, high temperature resistance solvents were needed, such as n-hexadecylamine (HDA), n-dodecylamine (DDA),

tri-*n*-octylamine (TOA), 1-hexadecanol (HD), 1-octadecene (OD) and purified mineral oil [45-47], and $\text{Zn}(\text{CH}_3\text{COO})_2 \cdot 2\text{H}_2\text{O}$ was used as precursors. Before putting Zn source into solvents, it was firstly dissolved in water or oleic acid (OA). The mixture was then heated up to a certain high temperature with stirring and kept for hours. After that, ZnO QDs were obtained by filtering, washing and drying. For synthesis taken place in air environment, instable zinc salts or instable zinc oxides were synthesized in solution or in air first [48-50]. After filtering and washing precipitation formed by mixing zinc source and oxygen source, as-obtained precursors of ZnO QDs were heated in air for hours until decomposition was completed.

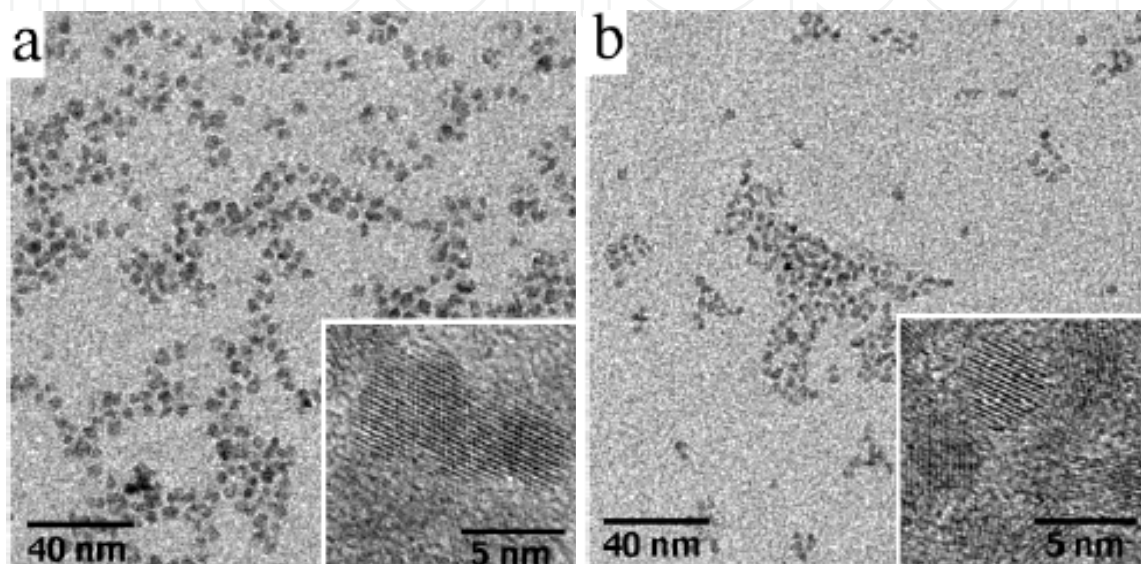


Fig. 3. TEM images of ZnO QDs prepared by thermal decomposition method: ZnO QDs prepared in *n*-hexadecylamine (HDA) with different molar ratio (*R*) of *tert*-Butylphosphonic acid (TBPA) and zinc acetate (ZnAc_2), (a) $R=0.12$ (b) $R=0.52$. In the inset, HR-TEM images show ZnO QDs with diameters less than 5nm. (Courtesy of P. D. Cozzoli et al [47])

4. Electrochemical growth method

Electrochemical growth method is a novel and simple method to fabricate ZnO QDs. Only a few reports have been shown up on it. Mahamuni and co-workers [51-54] have reported a lot of their work on synthesizing ZnO QDs using electrochemical growth method. Figure 4 shows TEM images of as-prepared ZnO QDs with average sizes of 6.1nm and 9.3nm [51].

In typical preparation of ZnO QDs, an electrochemical bath consisted of a mixture of acetonitrile, tetrahydrofuran (THF) and tetra-octyl-ammonium-bromide (TOAB). Metal zinc served as a sacrificial anode while platinum served as cathode. Electrolysis was taken for a few hours in constant current mode in oxygen ambient at room temperature. ZnO QDs deposited at the bottom of the electrochemical bath and then, were obtained after centrifugation.

Compared with most of other chemical methods for synthesis of ZnO QDs using OH-ion solution as the reagent, electrochemical growth method can effectively prevent ZnO QDs suffering from OH-ion. Otherwise, it is very easy for ZnO QDs to coat with a $\text{Zn}(\text{OH})_2$ layer to form ZnO/ $\text{Zn}(\text{OH})_2$ core/shell QDs or nanoparticles [88, 89]. The properties of ZnO QDs can be strongly influenced by $\text{Zn}(\text{OH})_2$ shell. Electrochemical growth method has provided a novel way to fabricate high quality ZnO QDs.

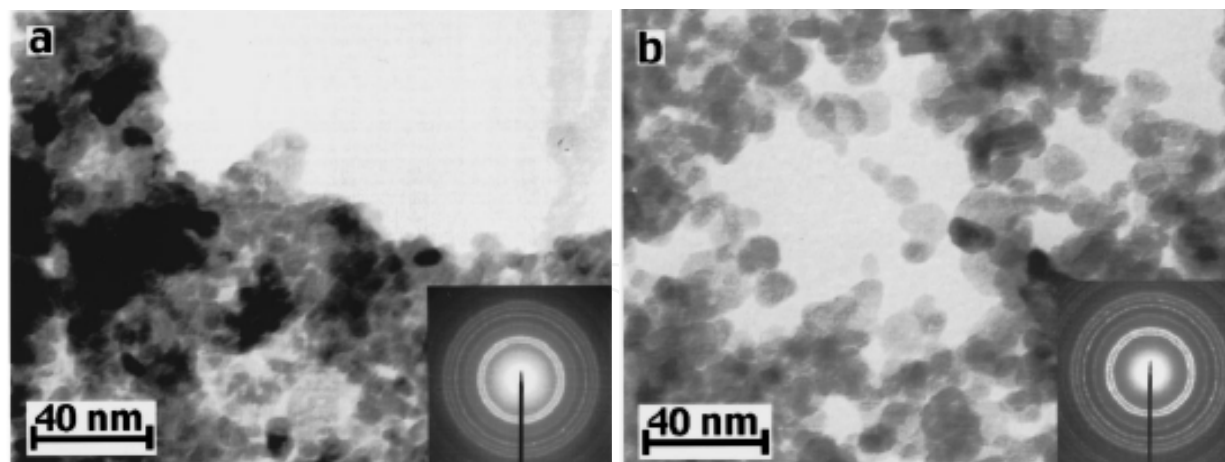


Fig. 4. Bright-field TEM images of: (a) 6.1 ± 2.0 nm and (b) 9.3 ± 3.1 nm ZnO QDs prepared by electrochemical growth method. Selected area diffraction patterns matching wurtzite ZnO are shown in the insets. (Courtesy of S. Mahamuni et al [51])

4. Physical methods on synthesis of ZnO QDs

1. Pulsed laser ablation (PLA or PLD)

Pulsed Laser Ablation is a novel technique to fabricate nanomaterials, which is based on ablating metals or metal compound materials using a laser with high pulsed power, [90-94]. The whole process can take place in either liquid environment or a vacuum chamber, known as Liquid-phase Pulsed Laser Ablation (LP-PLA or PLA) and Pulsed Laser Deposition (PLD), respectively.

Pulsed laser ablation method, which has been proven to be an effective method for fabrication of nano-sized metal QDs, including Au, Ag, Ti and Ni [90, 95-97], is also a promising method to fabricate QDs of compound semiconductors, such as FeO, ZnO, CdS and TiO₂ [55, 91, 92, 98]. Ajimsha et al [55] prepared ZnO QDs with an average size of 7 nm in various liquid media using PLA method (Figure 5).

In preparation of ZnO QDs, third harmonic of Nd:YAG laser (355 nm), amplified Ti:Sapphire laser (800 nm) and KrF excimer laser (248 nm) were usually used. A sintered ZnO bulk or a Zn metal plate was used as the target immersed in different liquid media like deionized water, methanol, and ethanol or in aqueous solutions with different surfactants like sodium dodecyl sulfate (SDS), HCl and NaOH. The target was rotated during the ablation to avoid repeated ablation on the same spot by continuous irradiation of the focused laser beam. ZnO QDs were finally dispersed in the liquid media or solution.

PLD was widely used in fabrication of thin film as many reports have been shown up over the last decade [94, 99, 100]. However, it has quite rarely reported fabrication of QDs because of aggregation. Barik et al [58] and Chen et al [59] have realized fabrication of ZnO QDs using PLD method. PLD method is quite similar to PLA method, whereas the only difference is the synthetic environment. Vacuum condition is needed in PLD process. The as-prepared ZnO QDs were finally deposited on the substrate fixed by the target source. Detailed study has demonstrated that the size of as-prepared ZnO QDs was influenced by the deposition time, ambient temperature and laser power.

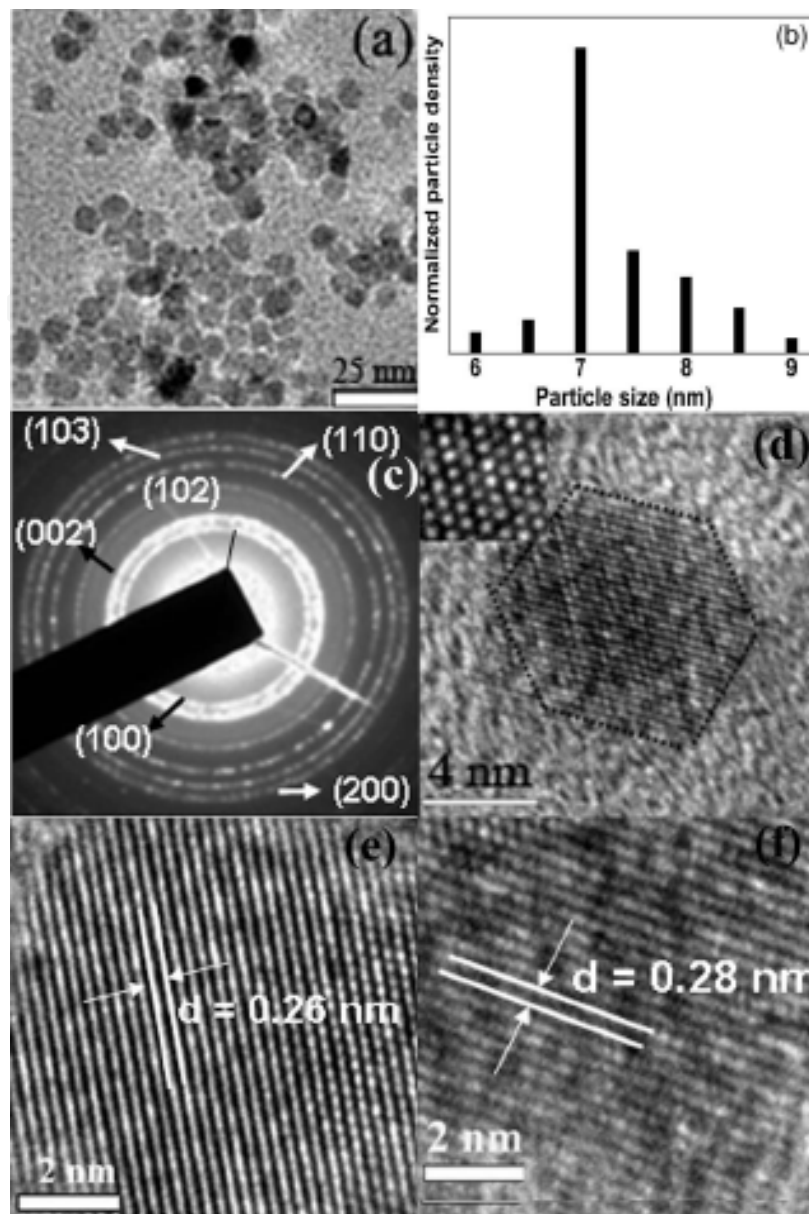


Fig. 5. TEM images and particle-size distribution of ZnO QDs prepared by PLA: (a) TEM image, (b) particle-size distribution, and (c) SAED pattern of ZnO QDs obtained by laser ablation with a fluence of 25 mJ/pulse in water. (d) HR-TEM image for a single QD and (inset) arrangement in the hexagonal close-packed mode. (e and f) HR-TEM showing (002) and (100) planes, respectively. (Courtesy of R. S. Ajimsha et al. [55])

2. Metalorganic chemical vapor deposition (MOCVD)

This method known as metalorganic chemical vapor deposition (MOCVD) is widely used in synthesis of various species of materials with different shapes, especially thin films or multilayer devices [101-103]. As nano-sized ZnO has attracted a lot of attention in the past decade, MOCVD also began to be used in fabricating ZnO nanostructures, such as nanowires, nanorods [104, 105]. However, there are not many reports on synthesis of ZnO QDs using MOCVD [60-63]. Tan et al [60] reported fabrication of ZnO QDs embedded films on Si substrates (Figure 6). Detailed study showed that with increasing substrate temperature, the diameters of QDs were increased with less dispersion.

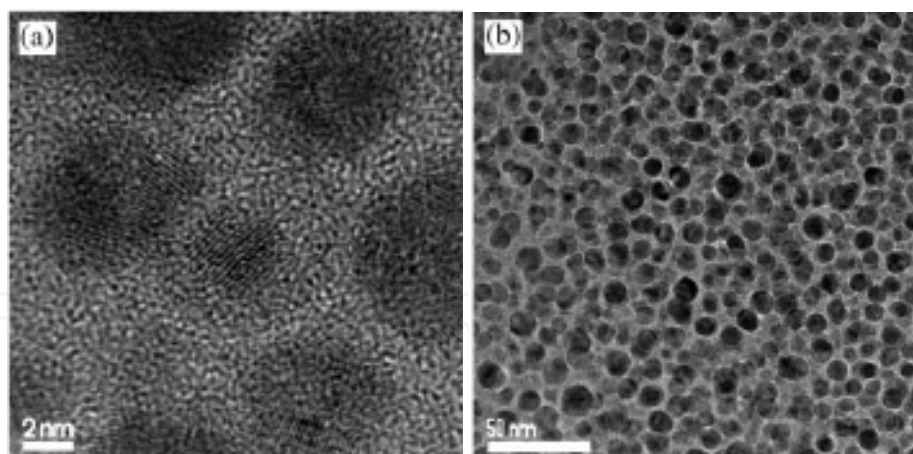


Fig. 6. TEM images of ZnO QDs prepared by MOCVD: (a) high magnification and (b) lower magnification of ZnO QDs embedded film fabricated on Si substrates. (Courtesy of S. T. Tan et al, [60])

In typical preparation of ZnO QDs, diethylzinc (DEZn) was chosen as the source of zinc, while the source of oxygen can be obtained from different gases, such as nitrous oxide (N_2O), nitrogen dioxide (NO_2) and oxygen (O_2). Nitrogen (N_2) was mostly employed as the carrier gas. However, most probably, there is a SiO_2 layer on the surface of the Si substrate due to oxidative environment at high temperature. Therefore, as-prepared ZnO QDs may be embedded in the SiO_2 layer or deposited on the SiO_2/Si substrate.

Kim et al [62, 63] reported fabrication of ZnO QDs assisted with focused ion-beam. Nano-sized patterns were made on the substrate by focused ion-beam and high aligned ZnO QDs were prepared along the pattern by MOCVD.

3. Radio frequency (RF) sputtering

Radio Frequency (RF) Sputtering is an effective method for preparation of thin films [106-108]. However, reports on preparation of QDs using RF sputtering is quite rare, mainly due to the aggregation of QDs on substrate which leads to form thin films. Recently, ZnO QDs embedded in SiO_2 and SiO_xN_y films were prepared via RF sputtering method by Peng et al [64, 65] and Ma et al [66].

In the preparation of ZnO QDs, high purity ZnO pieces were fixed at the certain distance from the substrate or directly on the substrate during sputtering. Si or Si_3N_4 were used as substrates in order to fabricate different ZnO QDs embedded films. The whole sputtering procedure was carried out in a low ambient pressure with a mixture of Ar and O_2 introduced into the chamber. After deposition, SiO_2 or SiO_xN_y film with ZnO QDs embedded were obtained on the substrates.

It was also reported that ZnO QDs embedded SiO_2 films were prepared by annealing ZnO thin films on SiO_2/Si substrates. The ZnO films were grown on Si substrates at room temperature by RF sputtering [109].

4. Flame spray pyrolysis (FSP) method

Flame spray pyrolysis (FSP) is a promising technique in flame-made technology. This method has been widely used in fabrication of many nano-sized materials including TiO_2 , ZrO_2 , Al_2O_3 , SiO_2 , SnO_2 , ZnO, CeO_2 QDs [110-116] and multicomponent oxide QDs, such as ZnO/ SiO_2 , $\text{TiO}_2/\text{Al}_2\text{O}_3$ and $\text{CeO}_2/\text{ZrO}_2$ [117-119]. In the FSP process, the heat generated from fuel combustion was used to decompose the metalorganic precursors. After decomposition, gas-phase metals rapidly react with oxygen to form metal oxide particles.

Over the past decade, Madler et al [68] has successfully fabricated ZnO QDs with diameter about 1.5nm using FSP method. Figure 7 shows HR-TEM images of as-prepared ZnO QDs [68].

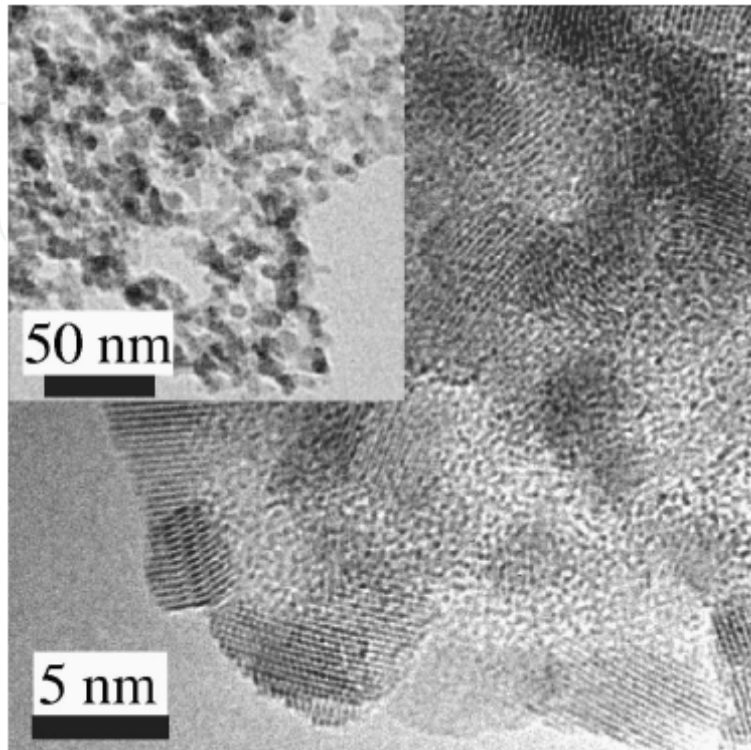


Fig. 7. ZnO QDs prepared by flame spray pyrolysis (FSP) method. (Courtesy of L. Madler et al. [68])

In typical preparation, zinc acrylate was chosen as zinc precursor and dissolved in the solvent, a mixture of acetic acid and methanol. As-obtained transparent solution was fed by a glass syringe into the oxygen-assisted atomizer nozzle, and then sprayed into the high temperature reaction zone which was surrounded by supporting flamelets. With the aid of a vacuum pump, the produced QDs were collected on a glass fiber filter. The highest temperature of the flame in the center was estimated to be above 2000K. ZnO was easily obtained from decomposing metalorganic precursors and reacting with oxygen.

Liewhiran et al [70] fabricated ZnO QDs with a diameter of 10-20nm which presented high performance in ethanol sensors. Against aggregation, reducing the precursor feed rate helps to decrease the diameter of ZnO QDs [68].

5. Vapor phase transport (VPT) deposition

The vapor phase transport (VPT) deposition process which needs very simple equipment has been extremely wide and successful used in fabricating nano-sized compound materials, including CdS, ZnS, ZnO, etc. [120-124]. The only equipment used in VPT process is a horizontal tube furnace with high-temperature capacity. ZnO nanomaterials have obtained great development via introducing this promising technique. The typical structures, such nanowires, nanorods or array of nanorods and nanobelts, have been realized in the past decade [122, 125-128]. 0D ZnO nanomaterials have been rarely reported until recently, Lu et al [71, 72] reported fabrication of ZnO QDs with controllable size using VPT process. Figure 8 shows as-prepared ZnO QDs with a diameter around 7nm [71].

In typical preparation, Zinc acetate dihydrate ($\text{Zn}(\text{CH}_3\text{COO})_2 \cdot 2\text{H}_2\text{O}$) was used as the zinc source, while two gases, O_2 and Ar, were input as oxygen source and carrier gas. A one-end-sealed quartz tube was used to hold source materials and Si substrates. The whole quartz tube was placed in a sealed horizontal tube furnace. High temperature was needed to decompose metalorganic to vaporize metals and react with oxygen. ZnO QDs were deposited at the low temperature zone where substrates were located.

Detailed study has been experimentally demonstrated that smaller size with better dispersion of ZnO QDs could be achieved by reducing the growth time at the highest temperature (Figure 8).

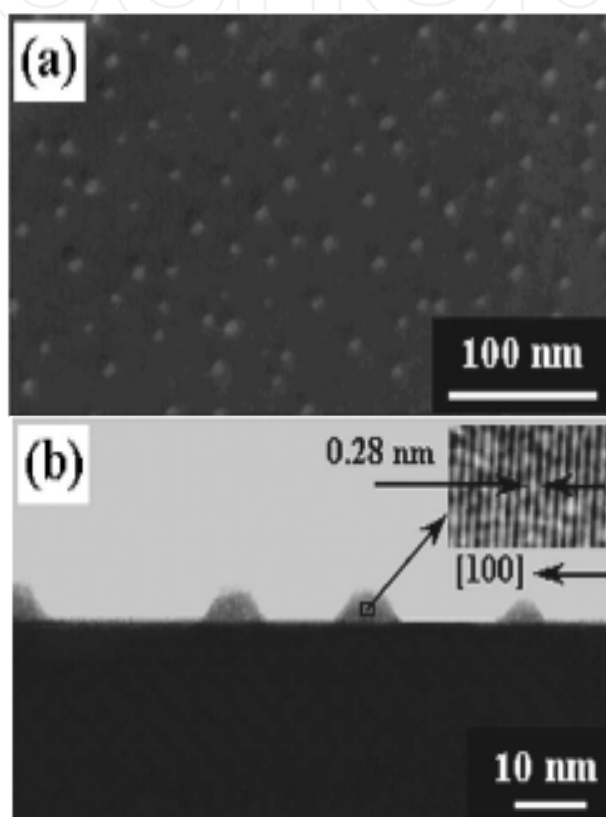


Fig. 8. (a) Plan-view and (b) cross-sectional TEM images of as-prepared ZnO QDs. An inset high-resolution TEM image shows that the ZnO QDs are single crystal. (Courtesy of J. G. Lu et al. [71])

5. Self-assembly of ordered 2D and 3D superlattices of ZnO QDs

ZnO is a luminescent, wide-band-gap semiconductor material that may find applications in a wide range of domains. However, many applications require the organization of the nanoparticles into two- or three-dimensional (2D or 3D) superlattices.[129] Recently, Bruno Chaudret and co-workers reported a study concerning the conditions governing the formation in solution and the dissolution of superlattices of ZnO QDs in the presence of long-alkyl-chain amines, carboxylic acids, or binary amine/carboxylic acid mixtures.[130-131]

The synthesis of ZnO QDs is carried out by slow hydrolysis in air of a THF solution containing the precursor ZnC_2Y_2 as well as one equivalent of a long-alkyl-chain amine and

half an equivalent of a long-alkyl-chain acid. Thus, when the reaction mixture was exposed to air and left withstanding room temperature, the solvent slowly evaporated, left with white and luminescent products. 2D organizations were spontaneously obtained by depositing one drop of the colloidal solution onto a carbon coated copper grid. Table 1 summarizes the results obtained under various reaction conditions and Figure 9 illustrates some examples of the materials obtained.

Ligand ^[a] (per mole ZnCy ₂)	Solvent	Nanoparticle size [nm] ^[b]
HDA/0.5 OcA	THF	3.5 ±1.0
HDA/0.5 OIA	THF	3.1 ±1.1
HDA/0.5 LcA	THF	2.8 ±0.8
DDA/0.5 OcA	THF	3.5 ±0.9
DDA/0.5 OIA	THF	3.5 ±1.7
DDA/0.5 LcA	THF	3.5 ±1.0
OA/0.5 OcA	THF	3.1±0.9
OA/0.5 OIA	THF	3.7±0.9
OA/0.5 LcA	THF	3.2±0.7
OA/0.5 OcA		3.6 ±1.1
OA/0.5 OIA		3.8 ±1.8
OA/0.5 LcA		3.7 ±1.4
2OA/0.5 OIA		3.6 ±1.4
5OA/0.5 OIA		3.4±1.5

Table 1. All procedures were carried out at room temperature, with an incubation time of 17 hours. The particles then were maintained in moist air for 4 days. For each experiment, the concentration of the zinc precursor was 0.042 M. [a]: HDA, DDA, OA, OcA, OIA, and LcA stand for hexadecylamine, dodecylamine, octylamine, octanoic acid, oleic acid, and lauric acid, respectively. [b]: The mean diameter of the obtained nanoparticle was evaluated by fitting of the histogram with a Gaussian curve. The first value corresponds to the centre of the peak whereas the second one corresponds to two times the standard deviation of the Gaussian distribution, or approximately 0.849 times the width of the peak at half height. (Courtesy of M. L. Kahn et al. [130])

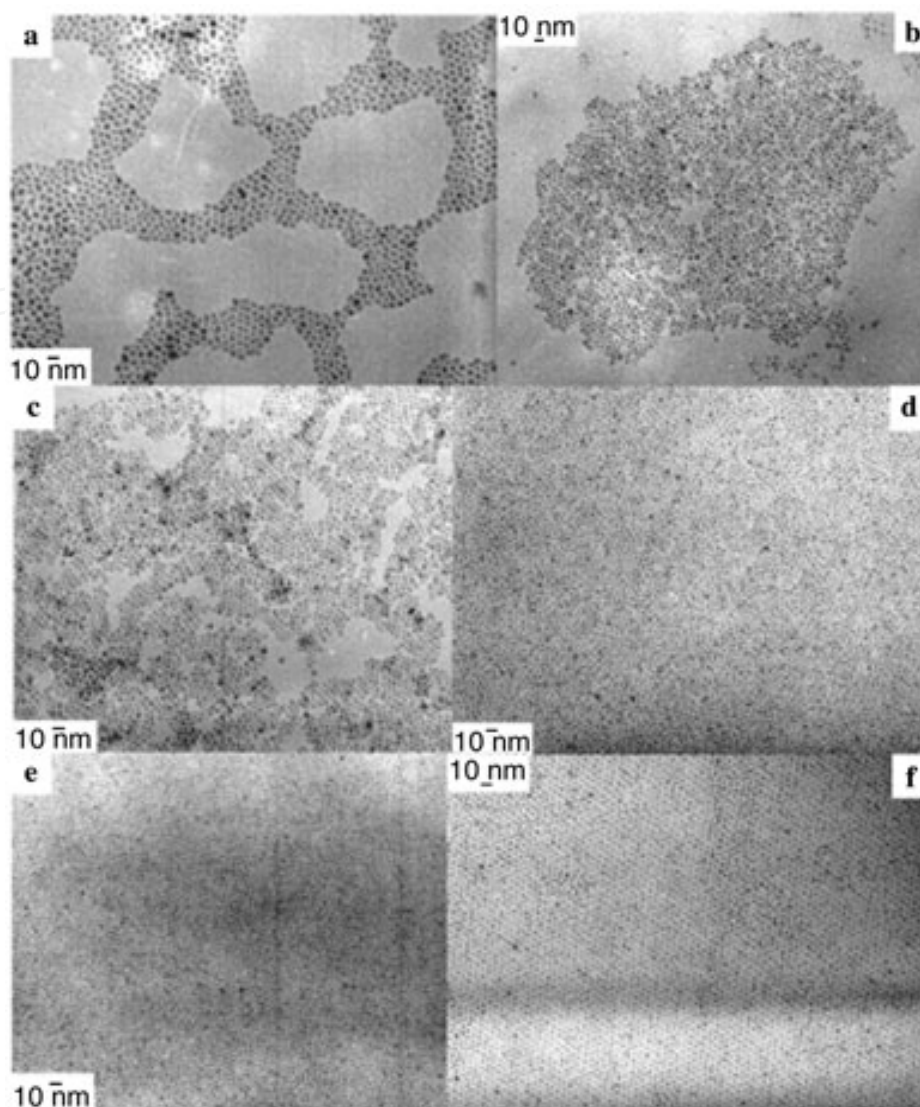


Fig. 9. TEM pictures of ZnO nanoparticles obtained in the presence of: a) OA and OIA (1:1) without other solvent; b) OA and OIA (2:1) without other solvent; c) OA and OIA (10:1) without other solvent; d) OA and LcA (1:1) in THF; e) DDA and OcA (1:1) in THF; f) HDA and OIA (1:1) in THF. (Courtesy of M. L. Kahn et al. [130])

3D superlattices were obtained through slow evaporation of colloidal THF solutions. The superlattices are not monodisperse in size but display uniform hexagonal shapes. Interestingly, this shape may be related to the intrinsic hexagonal crystallographic structure of ZnO, as previously observed for the organization of iron nanocubes.[132, 133] Figure 10 shows SEM image of small 3D superlattices of 3.1 nm ZnO nanoparticles obtained from HDA and OIA. Larger 3D superlattices may be obtained when crystallization is performed until the quasi-complete evaporation of the solvent.

In addition, Chen et al. [134] also reported that highly ordered, free-standing, complex, 2D or 3D nanoparticle superlattice arrays were created by either evaporation-induced self-assembly or precipitation-induced self-assembly from the size-monodispersed ZnO nanoparticles functionalized by carboxylic and alkylthiol ligands recently. The synthesis of the constituent ZnO nanoparticles is both novel and facile and is suggested as a generic means of producing oxide nanomaterials by reaction of metal cations and oxide anions in

alcohol solutions at room temperature. The regularity of the nanoparticle products and their chemical functionalization provides the means to achieve superlattice thin films on indium tin oxide (ITO)-coated glass slides (Figure 11).[134]

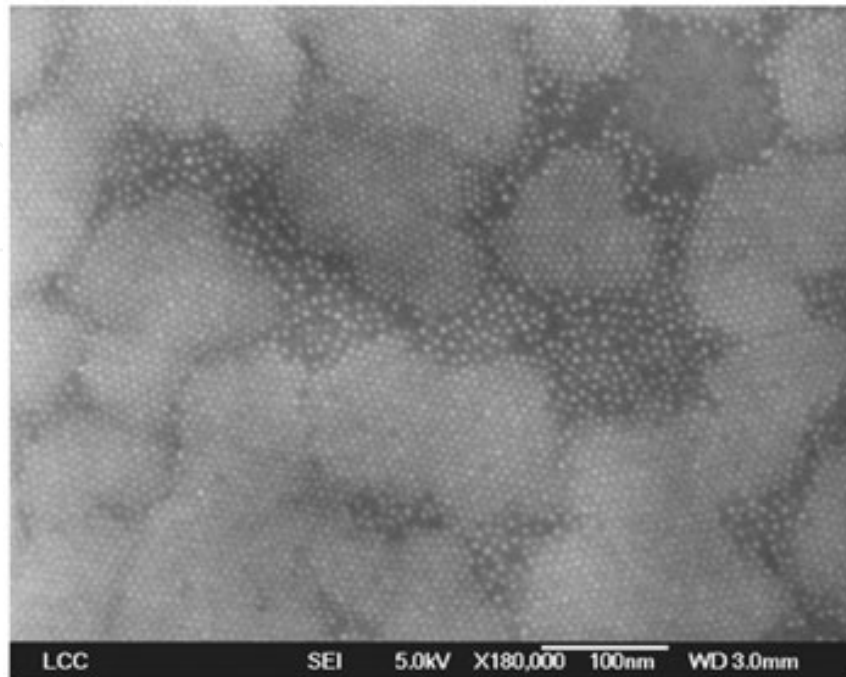


Fig. 10. SEM image of 3D superlattices of ZnO QDs prepared in the presence of HDA and OLA. (Courtesy of M. L. Kahn et al. [130])

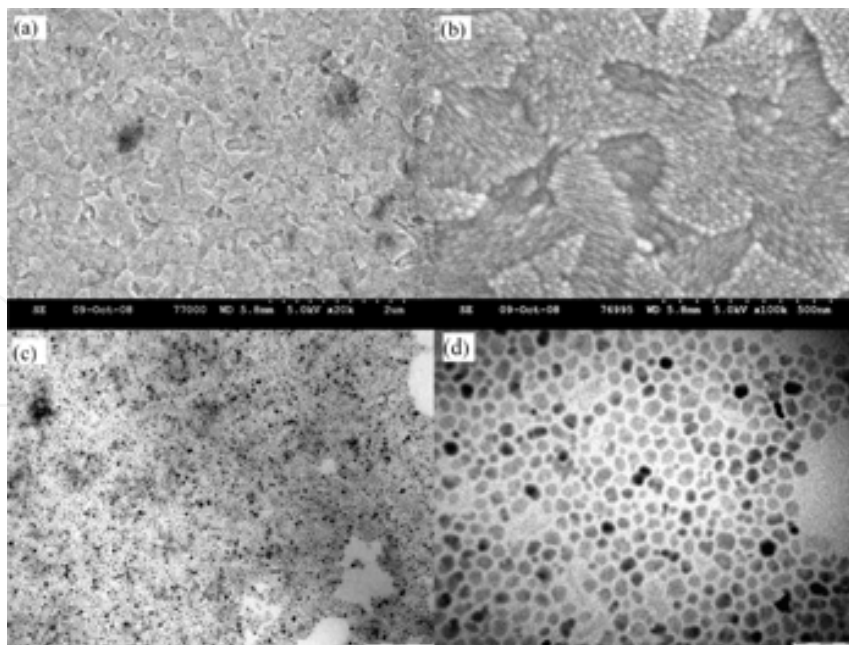


Fig. 11. EISA of OLA-ZnO QD superlattices. The (a) low- and (b) high-magnification SEM images of the layered 3D OLA-ZnO NP superlattice film and the (c) low- and (d) high-magnification TEM images of the 2D OLA-ZnO NP superlattice array self-organized on ITO slides. (Courtesy of L. Chen et al. [134])

The functionalization of these ZnO nanoparticles by long-chain carboxylic acids or alkylthiols improves the size monodispersity, and semiconduction properties dramatically. The 2D or 3D self-assembly process is driven by the interfacial energy minimization between polar solvents and the hydrophobic moieties of OLA-ZnO NPs where well-organized, ordered nanoparticle superlattice structures are produced by either evaporation-induced self-assembly (EISA) or precipitation-induced self-assembly (PISA).

6. ZnO QDs optoelectronic properties and application

1. The Photoluminescence and Bandgap of ZnO QDs

The photoluminescence (PL) spectrum of the as-prepared ZnO QDs sample reported by Hu et al. [41], was measured at room-temperature with the excitation at a wavelength of 325 nm, as shown in Figure 12. A strong UV light emission peak is clearly observed at 362 nm, corresponding to transition energy of 3.42 eV. A remarkable blue shift of 0.16 eV with respect to the gap energy (3.26 eV) of bandedge emission of bulk ZnO crystals is obtained due to the quantum confinement effect in ZnO QDs. [135] The corresponding band-gap energy is larger than the emission peak energy by the excitonic binding energy. Such an enlarged band gap implies a diameter of 3.5 nm of QDs.[136]

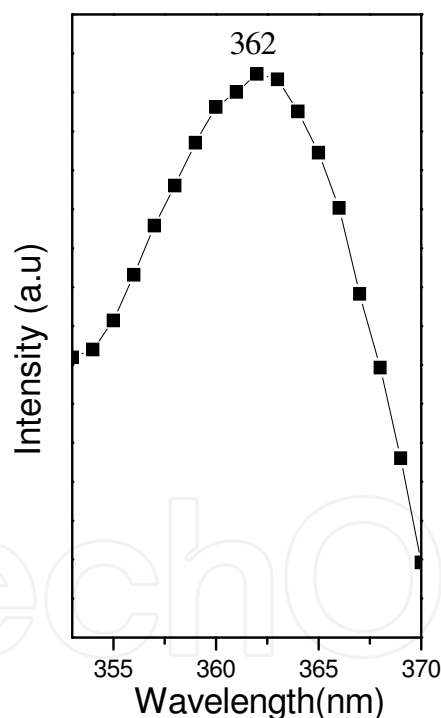


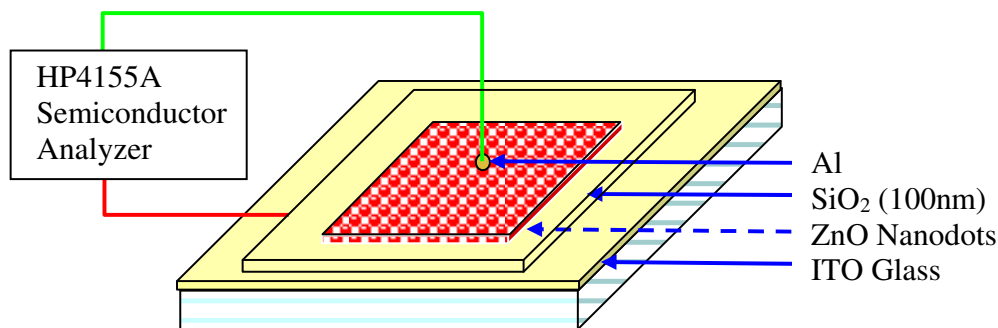
Fig. 12. PL spectrum of ZnO nanocrystals ($\lambda_{\text{ex}}=325\text{nm}$). [41]

The ZnO nanodots were assembled into an ITO/ZnO/SiO₂/Al structure (see Scheme 1) in order to further determine the band alignment of ZnO nanodots on ITO via analysis of I-V characteristics. Figure 13 presents the band diagrams of the ITO/ZnO/SiO₂/Al structure under the two opposite biases. Due to high barriers in both conduction and valence bands at the Al/SiO₂ interface, electron and hole injections from the SiO₂ end were negligible. This is evidenced by the experimental result that the current ratio of ITO/ZnO/SiO₂/Al to ITO/SiO₂/Al is about 100. Figure 14a shows the forward biased I-V characteristics of these

two structures. Therefore, we can consider unipolar carrier injection in the ITO/ZnO/SiO₂/Al structure. For sufficiently high bias as illustrated in Figure 13, holes or electrons may tunnel through the ZnO nanodot layer and contribute an appreciable current that follows the Fowler-Nordheim (FN) tunneling equation [137, 138]

$$I_{\text{FN}} = C_{\text{FN}} E^2 \exp\left(-\frac{4}{3} \frac{(2m^*)^{1/2} \phi^{3/2}}{eh E}\right),$$

where I_{FN} is the current, E is the electric field across oxide, m^* is the electron or hole effective mass, e is the electronic charge, \hbar is the reduced Planck's constant, and ϕ is the barrier height. As shown in Figure 14b and c, the FN plots $\ln(I/E^2)$ vs. $1/E$ at high electric field show a good linearity as the sign of the FN tunneling mechanism. The slopes of -2×10^{10} and -3×10^9 can be determined from the linear regions in forward bias and reverse bias, respectively. Apart from the linear regions, other current injection mechanisms may be dominant, e.g. space charge limited current, etc.. Given effective masses m_h^* ($=0.59m_0$) and m_e^* ($=0.19m_0$) for hole and electron,[139, 140] the barrier heights are calculated to be 2.44eV and 1.0 eV, indicating the band alignment of the ZnO nanodots on ITO. The barrier heights sum up to be 3.44eV, which agrees to the value of the band gap of ZnO nanodots derived from the PL test very well.



Scheme 1. The fabrication of ITO/ZnO/SiO₂/Al structure

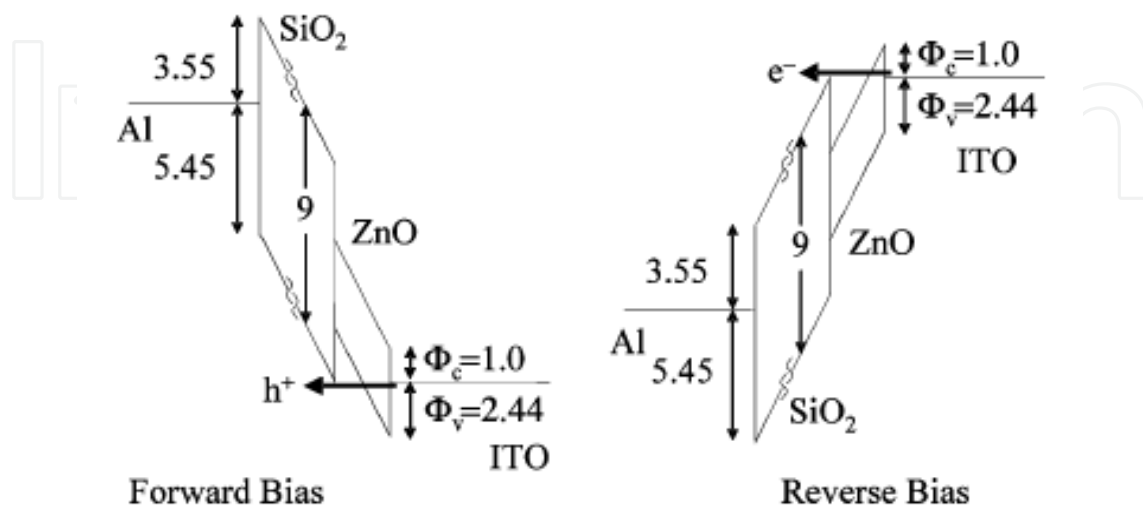


Fig. 13. Energy band diagrams for the ITO/ZnO/SiO₂/Al structure biased under a high field showing hole and electron tunneling, respectively. [41]

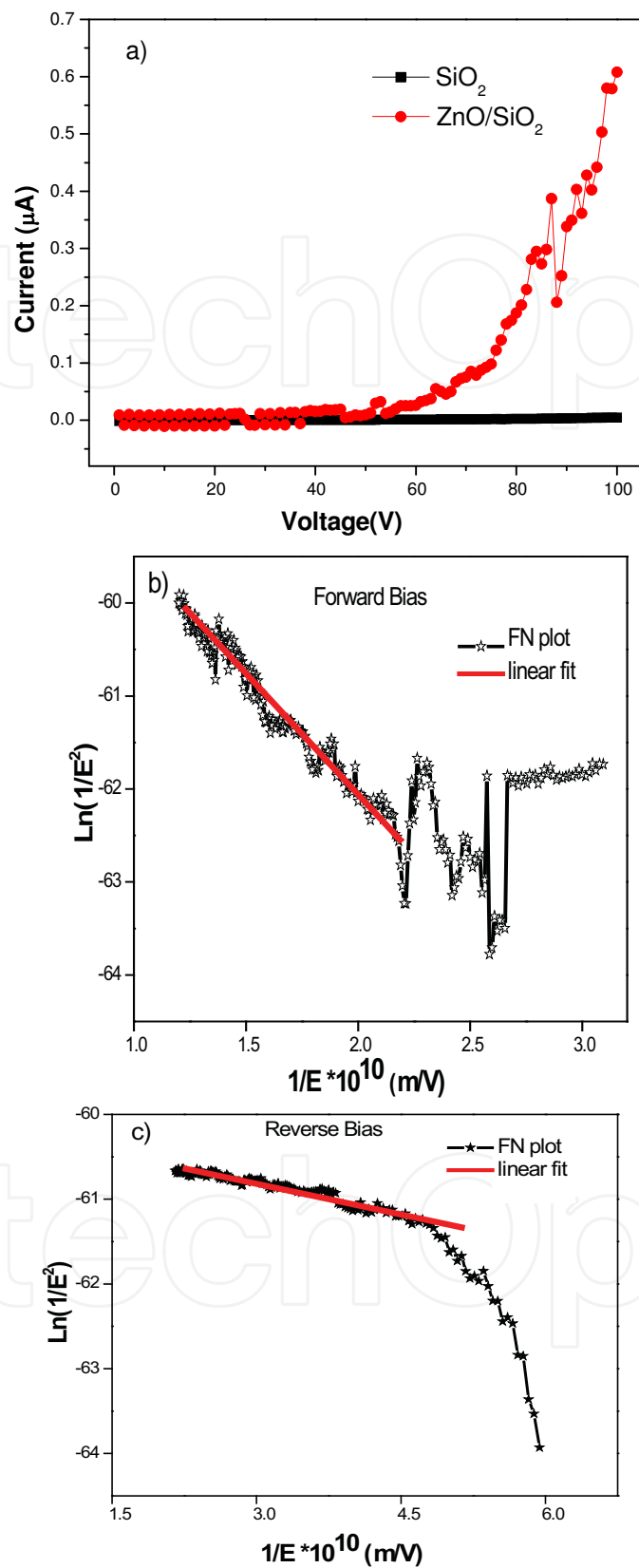


Fig. 14. a) I-V characteristics of the ITO/ZnO/SiO₂/Al and the ITO/SiO₂/Al structures at forward bias; and Fowler-Nordheim (FN) plots for the ITO/ZnO/SiO₂/Al structure at b) forward biases and c) reverse biases. [41]

2. The Electroluminescence of monolayer ZnO nanoparticles

Ultraviolet electroluminescence from ZnO nanoparticle-based devices prepared by the dry-coating technique has been investigated by Lee et al. This section was developed based on their report [141].

With dry-coating process, the structure of the ZnO nanoparticle monolayer (90 nm) in the device can be easily achieved. The method reduces the density of pinhole defects in the ZnO nanoparticles. In this work, they prepared three types of ZnO EL devices formed with a host polymer, ZnO nanoparticle monolayer, and an electron transporting layer. The following host matrix materials dissolving in chloroform with different concentration are chosen respectively: 0.7 wt % poly(fluorine) (PF), 1 wt % poly(*N*-vinylcarbazole) (PVK), and 0.7 wt % poly(3-hexylthiophene) (P3HT). For the electron transporting layer, they employed small-molecular aluminum tris-8-hydroxyquinoline (Alq3). The ZnO nanoparticles were purchased from Aldrich.

The device structure is ITO/host matrix/ZnO nanoparticles (monolayer)/Alq3/Al. The schematic of the device structure is shown in Figure 15a. In order to get the optimized film-forming property, the different host matrixes have the different thickness by different spin-coating condition (PF: 200 nm, PVK: 900 nm, and P3HT: 110 nm). These samples are baked at 170 °C (device I), 170 °C (device II), and 120 °C (device III) for 2 h individually. In addition, in order to reduce the density of pinhole defects in ZnO nanoparticles, the dry-coating technique is used for development of the ZnO nanoparticles monolayer. During the dry-coating process, the ZnO nanoparticles are adsorbed on the host matrix using ZnO nanoparticle smog during dry-coating process. The ZnO nanoparticle smog is making by homemade nanosmog-making machine, as shown schematically in Figure 15b.

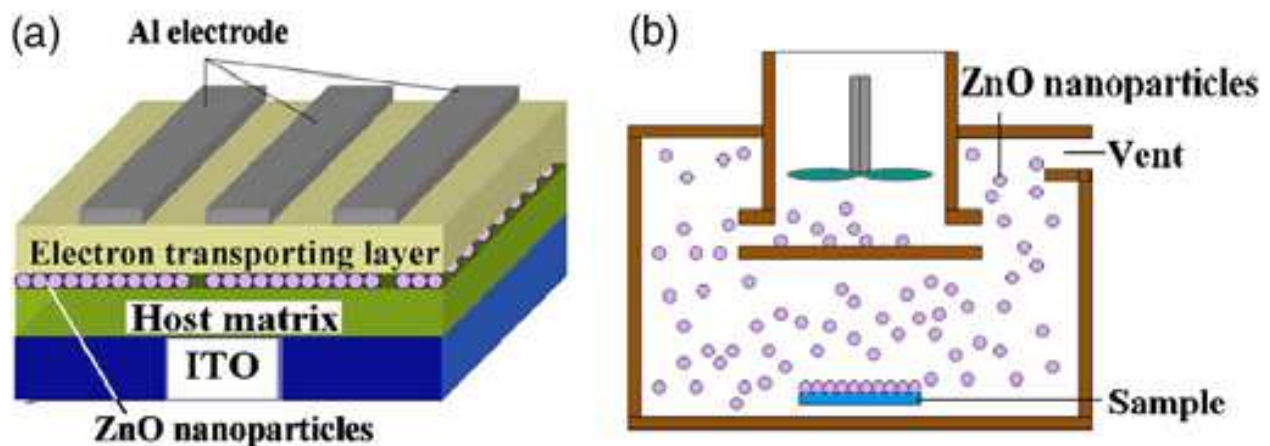


Fig. 15. a) Cross-sectional schematic of the ZnO EL device structure; b) The schematic of the dry-coating machine. (Courtesy of C. Y. Lee et al. [141])

The EL characteristics of the ZnO nanoparticle devices are also measured. Figure 16a shows the EL spectra of the three kinds of the ZnO nanoparticle devices under forward bias of 9 V. For the device with PF (device I, curve a), the EL spectrum shows a strong ZnO band-gap emission peak at 380 nm with the broad background emission from PF. The full width at half maximum of the spectrum is 100 nm. For the device with PVK (device II, curve b), it shows a broadband spectrum from 380 to 700 nm, which are the characteristics of the emissions of the ZnO nanoparticles (380 nm) and PVK (553 nm). The emissions indicate that the radiative recombination occurs in the ZnO nanoparticles and at the host matrix/Alq3

interface. For the device with P3HT (device III, curve c) at the same forward bias of 9 V, it also has a peak around 380 nm contributed from ZnO. To investigate the origin of the EL band, PL spectra of host matrix/ ZnO nanoparticles excited using the 266 nm of a Nd-YAG (yttrium aluminum garnet) laser are also measured at room temperature and shown in Figure 16b. For the device with the higher-energy host matrix (PF/PVK), the PL spectra show the emission band in the ZnO band-gap emission (380 nm) with a weak emission band from the host matrix. For the device with the lower-energy host matrix (P3HT), the PL spectrum shows the decreased ZnO band-gap emission and the strong host matrix emission, which is due to the Förster energy transfer from the higher-energy ZnO to the lower-energy host matrix. Thus, the ZnO EL device with the lower-energy host matrix causes the poor ZnO band-gap emission.

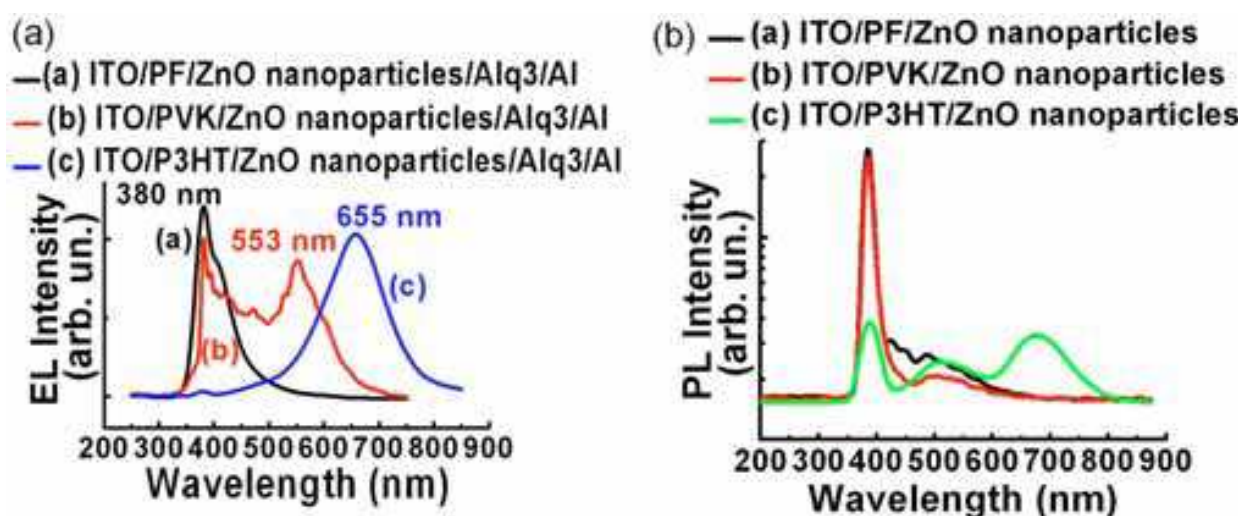


Fig. 16. a) Comparison of EL spectra of ZnO-based nanocomposites with different host matrixes, b) Room temperature PL spectra of three host matrixes (PF, PVK, and P3HT) with ZnO nanoparticles (The intensities are plotted in logarithmic scale, in order to distinguish from the different intensities of the different samples clearly). (Courtesy of C. Y. Lee et al. [141])

7. ZnO QDs for a nanophotonic signal transmission device

Recently, Yatsui et al reported a self-assembly method that aligns nanometer-sized QDs into a straight line. Photonic signals can be transmitted along the QD line by near-field optical effects. This section was developed based on their report [144].

Innovations in optical technology are required for continued development of information processing systems. One potential innovation, the increased integration of photonic devices, requires a reduction in both the size of the devices and the amount of heat they generate. Chains of closely spaced metal nanoparticles that can convert the optical mode into nonradiating surface plasmonic waves have been proposed as a way to meet these requirements.[142, 143] ZnO QDs were bound electrostatically to DNA to form a one-dimensional QD chain. The photoluminescence intensity under parallel polarization excitation along the QDs chain was much greater than under perpendicular polarization excitation, indicating an efficient signal transmission along the QD chain. As optical near-field energy can transmit through the resonant energy level, nanophotonic signal

transmission (NST) devices have a number of potential applications, such as wavelength division multiplexing using QDs of different sizes. [144]

To observe the optical properties of the NST, they stretched and straightened the QD-immobilized DNA on the silicon substrate using the molecular combing technique (Figure 17a). [145] First, the silicon substrate was terminated with the silane coupling agent so that the anionic DNA was adsorbed on the cationic silicon substrate. Second, the solution including the DNA and the QDs was dropped onto the cationic silicon substrate. Finally, the glass substrate was slid over the droplet. To check the alignment of DNA-QDs alignment, they obtained an emission image of the cyanine dye attached to the DNA using its 540 nm emission peak under halogen lamp illumination. As shown in the optical image taken with a charge-coupled device camera (Figure 17b), the DNA with QDs stretched in the direction determined by the slide direction of the glass substrate; also, these stretched DNA were found to be isolated.

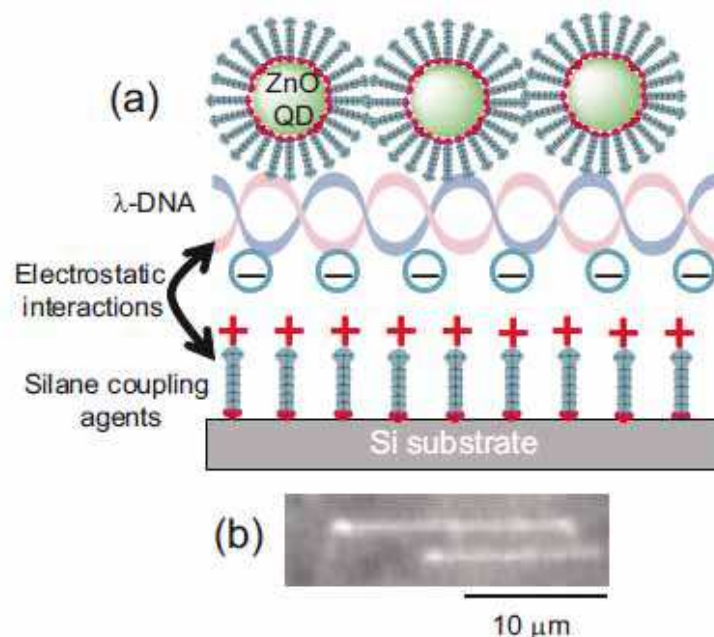


Fig. 17. Schematic of the molecular combing technique: (a) Schematic of the alignment of the DNA with QDs on the cationic silicon substrate. (b) Charge-coupled device image of the stretched λ -DNA. (Courtesy of T. Yatsui et al. [144])

Using the linearly aligned ZnO QDs, they evaluated the PL polarization dependence. A fourthharmonic of a Q-switched Nd:YAG laser (neodymium-doped yttrium aluminum garnet; Nd:Y₃Al₅O₁₂ laser, $\lambda=266$ nm) with a spot size of approximately 2 mm was used to excite the ZnO QDs at various polarization angles (Figure 18a). From the polarization dependence of the PL at a wavelength of 350 nm (Figure 18b), corresponding to the ground state of 5 nm ZnO QDs, stronger PL emission was obtained by exciting the parallel polarization along the QD chains (E_0) than was obtained under the perpendicular polarization (E_{90} ; Figure 18c). Since the decay time of ZnO QDs is more than 20 times longer than the energy transfer time to adjacent QDs,[146] it is possible that the dipoles between adjacent QDs were coupled by an optical near-field interaction, indicating that the signals were transmitted through the QD chain. Furthermore, QD chains have great dipolar

strength (see the inset of Figure 18c) that can be realized when the QDs are coherently coupled.[147, 148] If M QDs are coherently coupled and the coherent length along the z -axis is N times greater than that along the x -axis, the equivalent total dipolar strength is given by $Me \times d$ (E_{90} ; see Figure 18d) and $Me \times Nd$ (E_0 ; see Figure 18e), where e is the electrical charge excited in the QD and d is the coherent length along the x -axis, which is equivalent to the width of the QD chain. The resulting emission intensities are $(Me \times d)^2$ and $(Me \times Nd)^2$ for E_{90} and E_0 , respectively. Therefore, we obtained N^2 times greater PL intensity with E_0 than with E_{90} .

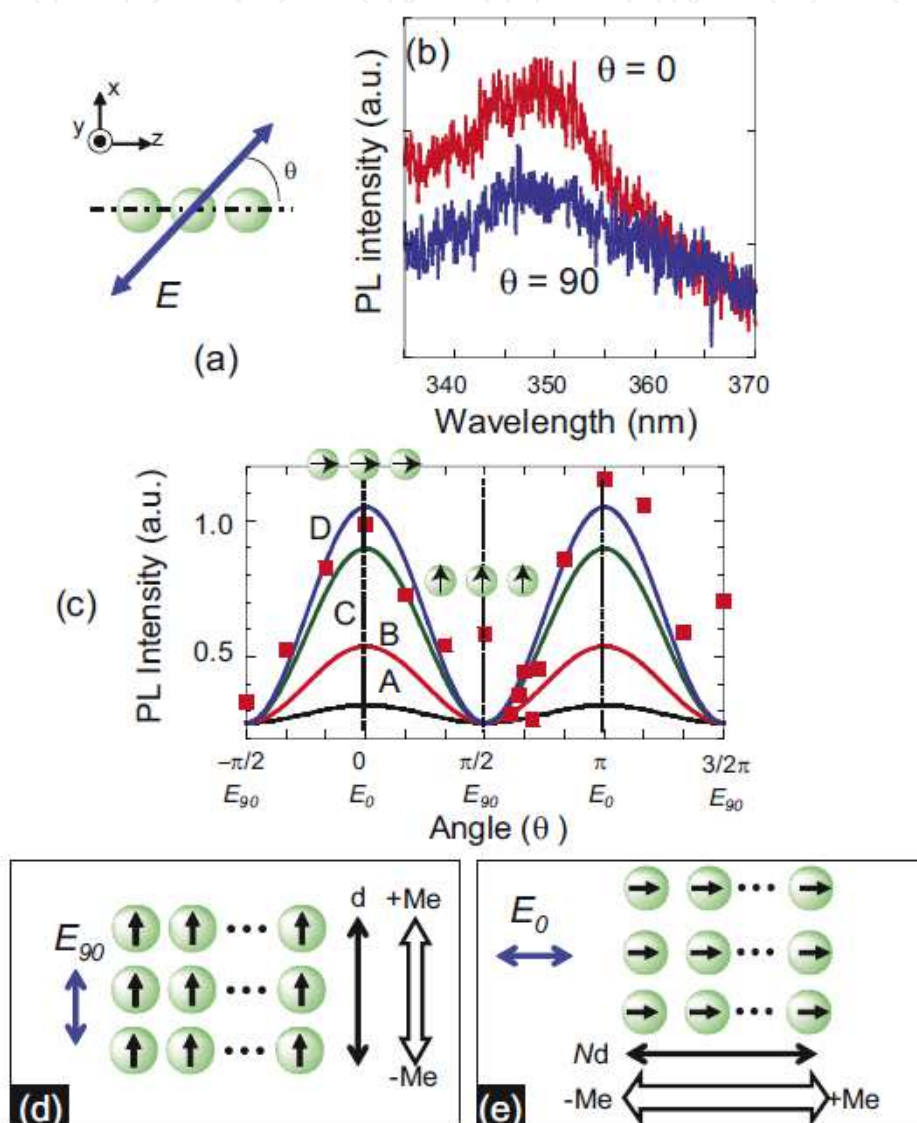


Fig. 18. Polarization dependence of the linearly aligned QD chain: (a) Incident light polarization dependence of PL intensity. θ : Polarization angle with respect to the direction along the QD chains (x -axis), (b) Typical PL spectra obtained at $\theta = 0$ and 90 . (c) Incident light polarization dependence of the PL intensity obtained at $\lambda = 350$ nm. Curves A to D correspond to $N = 3, 6, 9$, and 10 , respectively. Schematics of the equivalent total dipole strength under (d) E_{90} and (e) E_0 . (Courtesy of T. Yatsui et al. [144])

The polarization-dependent PL from the QD chain revealed that the coherent length along the QDs chain was 150 nm, indicating efficient signal transmission through the QD chain.

As optical near-field energy can transmit through the resonant energy level, NST devices have a number of potential applications, such as wavelength division multiplexing using QDs of different sizes.

8. Summary

This chapter describes most of the synthetic methods for synthesis of ZnO QDs. They are frequently used and experimentally demonstrated to be effective on synthesis of ZnO QDs. This chapter also clearly shows that the formation of ZnO superlattices in solution does not result from a kinetic condensation of particles but from a thermodynamic equilibrium. This may be compared to a molecular crystallization process in which an increase in concentration leads to generation of crystals whereas dilution leads to dissolution of them. The system is indeed complex, since several species are involved in the stabilization of the ZnO nanoparticles, and that these species are in thermodynamic equilibrium. Furthermore, we described in detail the origin of UV PL in ZnO QDs, discussing recombination of confined excitons or surface-bound acceptor–exciton complexes, a PL peak with a blue shift of 0.16 eV has been observed in the PL spectrum, showing good size uniformity of nanocrystals. The band gap has also been verified in the analysis of I-V characteristics of an ITO/ZnO/SiO₂/Al structure, high bias, holes or electrons may tunnel through the ZnO nanodot layer and contribute an appreciable current that follows the Fowler-Nordheim (FN) tunneling equation, from which the band alignment of the ZnO nanodots on ITO has been determined. This work demonstrates an efficient synthesis of nanodots and an easy approach to studying physical properties of nanocrystals that will help the material optimization in device application. This chapter also outlines the application of ZnO QDs optoelectronic property, such as EL and NST device. The results described in this chapter are important for the future development of ZnO technology and optoelectronic applications.

9. Acknowledgments

The authors gratefully acknowledge the financial support the Singapore National Research Foundation under CRP Award No. NRF-G-CRP 2007-01, T. Mei acknowledges support from Department of Education of Guangdong Province, China (Grant No. C10131). Y. Hu acknowledges support from the Educational Commission of Zhejiang Province of China (Grant No. Z200909406) and Zhejiang Qianjiang Talent Project (2010R10025).

10. References

- [1] M. Haase, H. Weller, A. Henglein. *J Phys. Chem.* 1998, 92, 482
- [2] E. M. Wong, P. C. Searson. *Appl. Phys. Lett.* 1999, 74, 2939
- [3] J. M. Klostranec, W. C. W. Chan. *Adv. Mater.* 2006, 18, 1953
- [4] S. A. Mcdonald, G. Konstantatos, S. G. Zhang, et al. *Nature Materials.* 2005, 4, 138
- [5] A. J. Nozik. *Physica E.* 2002, 14, 115
- [6] E. T. Kim, A. Madhukar, Z. M. Ye, et al. *Appl. Phys. Lett.* 2004, 84, 3277
- [7] S. Fafard, K. Hinzer, S. Raymond, et al. *Science.* 1996, 274, 1350
- [8] C. A. Leatherdale, W. K. Woo, F. V. Mikulec, et al. *J Phys. Chem. B.* 2002, 106, 7619
- [9] S. F. Wuister, I. Swart, F. V. Driel, et al. *Nano Lett.* 2003, 3, 503

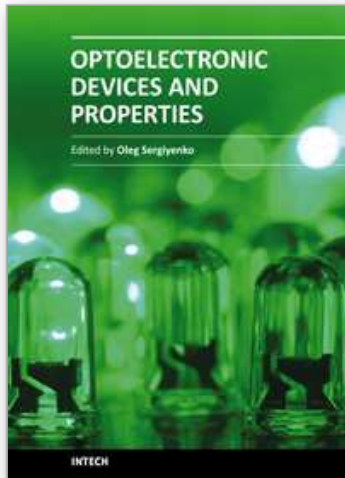
- [10] S. I. Erlingsson, Y. V. Nazarov, V. I. Fal'ko. *Phys. Rev. B*. 2001, 64, 195306
- [11] O. B. Shchekin, D. G. Deppe. *Appl. Phys. Lett.* 2002, 80, 3277
- [12] O. I. Micic, S. P. Ahrenkiel, A. J. Nozik. *Appl. Phys. Lett.* 2001, 78, 4022
- [13] M. A. Malik, P. O'Brien, N. Revaprasadu. *J Mater. Chem.* 2001, 11, 2382
- [14] Y. L. Wu, C. S. Lim, S. Fu, et al. *Nanotechnology*. 2007, 18, 215604
- [15] B. Capoen, A. Martucci, S. Turrell, et al. *J Molecular Structure*. 2003, 651, 467
- [16] W. Y. Mao, J. Guo, W. L. Yang, et al. *Nanotechnology*. 2007, 18, 485611
- [17] D. S. Wang, T. Xie, Q. Peng, et al. *Chem. Eur. J* 2008, 14, 2507
- [18] A. Iwabuchi, C. K. Choo, K. Tanaka. *J Phys. Chem. B*. 2004, 108, 10863
- [19] R. M. Laine, J. C. Marchal, H. P. Sun, et al. *Nature Materials*. 2006, 5, 710
- [20] B. Ludolph, M. A. Malik, P. O'Brien, et al. *Chem. Commun.* 1998, 1849
- [20] O. I. Micic, S. P. Ahrenkiel, D. Bertram, et al. *Appl. Phys. Lett.* 1999, 75, 478
- [21] J. G. Cederberg, F. H. Kaatz, R. M. Biefeld. *J Crystal Growth*. 2004, 261, 197
- [22] D. M. Bagnall, Y. F. Chen, Z. Zhu, et al. *Appl. Phys. Lett.* 1997, 70, 2230
- [23] D. C. Look. *Materials Science and Engineering B*. 2001, 80, 383
- [24] S. Krishnanoorthy, T. Bei, E. Zoumakis, et al. *Biosens. Bioelectron.* 2006, 22, 707
- [25] L. P. Bauermann, J. Bill, F. Aldinger. *J Phys. Chem. B*. 2006, 110, 5182
- [26] L. Spanhel, M. A. Anderson. *J Am. Chem. Soc.* 1991, 113, 2826
- [27] M. S. Tokumoto, S. H. Pulcinelli, C. V. Santilli, et al. *J Phys. Chem. B* 2003, 107, 568
- [28] H. K. Yadav, K. Sreenivas, V. Gupta, et al. *J Mater. Res.* 2007, 22, 2404
- [29] E. A. Meulenkamp. *J Phys. Chem. B* 1998, 102, 7764
- [30] D. W. Bahnemann, C. Kormann, M.R. Hoffmann. *J Phys. Chem.* 1987, 91, 3789
- [31] N. S. Pesika, Z. Hu, K. J. Stebe, et al. *J Phys. Chem. B* 2002, 106, 6985
- [32] E.M. Wong, J.E. Bonevich, P.C. Searson. *J Phys. Chem. B* 1998, 102, 7770
- [33] L. Guo, S. Yang, C. Yang, et al. *Appl. Phys. Lett.* 2000, 76, 2901
- [34] Z. Hu, G. Oskam, P. C. Searson. *J Colloid Interface Sci.* 2003, 263, 454
- [35] S. H. Li, M. S. Toprak, Y. S. Jo, et al. *Adv. Mater.* 2007, 19, 4347
- [36] K. F. Lin, H. M. Cheng, H. C. Hsu, et al. *Appl. Phys. Lett.* 2006, 88, 263117
- [37] K. F. Lin, H. M. Cheng, H. C. Hsu, et al. *Chemical Physics Letters*. 2005, 409, 208
- [38] M. Vafaei, M. S. Ghamsari. *Mater.Lett.* 2007, 61, 3265
- [39] R. Viswanatha, P. K. Santra, C. Dasgupta, et al. *Phys. Rev. Lett.* 2007, 98, 255501
- [40] Z. Hu, D. J. E. Ramirez, B. E. H. Cervera, et al. *J Phys. Chem. B* 2005, 109, 11209
- [41] Y. Hu, Z. M. Jiang, C. D. Xu, et al. *J Phys. Chem. C* 2007, 111, 9757
- [42] Y. Hu, T. Mei, J. Guo, et al. *Inorg. Chem.* 2007, 46, 11031
- [43] K. Sue, K. Kimura, K. Arai. *Mater. Lett.* 2004, 58, 3229
- [44] P. M. Aneesh, K. A. Vanaja, M. K. Jayaraj. *Proc. SPIE*. 2007, 6639, 66390J
- [45] T. Andelman, Y. Y. Gong, M. Polking, et al. *J Phys. Chem. B*. 2005, 109, 14314
- [46] I. D. Kosobudsky, N. M. Ushakov, G. Y. Yurkov, et al. *Inorg. Mater.* 2005, 41, 1172
- [47] P. D. Cozzoli, M. L. Curri, A. Agostiano, et al. *J Phys. Chem. B*. 2003, 107, 4756
- [48] L. L. Yang, J. H. Yang, X. Y. Liu, et al. *J. Alloys Compd.* 2008, Article in press
- [49] Y. C. Zhang, X. Wu, X. Y. Hu, et al. *J Crystal Growth*. 2005, 280, 250
- [50] L. M. Shen, L. C. Guo, N. Z. Bao, et al. *Chem. Lett.* 2003, 32, 826
- [51] S. Mahamuni, K. Borgohain, B. S. Bendre, et al. *J Appl. Phys.* 1999, 85, 2861
- [52] B. S. Bendre, S. Mahamuni. *J Mater. Res.* 2004, 19, 737
- [53] M. Rajalakshmi, A. K. Arora. *J Appl. Phys.* 2000, 87, 2445
- [54] S. D. Kshirsagar, V. V. Nikesh, S. Mahamuni. *Appl. Phys. Lett.* 2006, 89, 053120

- [55] R. S. Ajimsha, G. Anoop, A. Aravind, et al. *Electrochemical. Solid-State Lett.* 2008, 11, K14
- [56] A. Said, L. Sajti, S. Giorgio, et al. *J Phys :Conference Series.* 2007, 59, 259
- [57] H. Usui, Y. Shimizu, T. Sasaki, et al. *J Phys. Chem. B.* 2005, 109, 120
- [58] S. Barik, A. K. Srivastava, P. Misra, et al. *Solid State Commun.* 2003, 127, 463
- [59] L. Chen, Z. Q. Chen, X. Z. Shang, et al. *Solid State Commun.* 2006, 137, 561
- [60] S. T. Tan, X. W. Sun, X. H. Zhang, et al. *J Crystal. Growth.* 2006, 290, 518
- [61] L. M. Yang, Z. Z. Ye, Y. J. Zeng, et al. *Solid State Commun.* 2006, 138, 577
- [62] S. W. Kim, M. Ueda, M. Funato, et al. *J Appl. Phys.* 2005, 97, 104316
- [63] S. W. Kim, S. Fujita, S. Fujita, et al. *Appl. Phys. Lett.* 2002, 81, 5036
- [64] Y. Y. Peng, T. E. Hsieh, C. H. Hsu. *Appl. Phys. Lett.* 2006, 89, 211909
- [65] Y. Y. Peng, T. E. Hsieh, C. H. Hsu. *J Mater. Res.* 2008, 23, 1155
- [66] J. C. Ma, Y. C. Liu, C. S. Xu, et al. *J Appl. Phys.* 2005, 97, 103509
- [67] T. Tani, L. Madler, S. E. Pratsinis. *J Nanoparticle. Res.* 2002, 4, 337
- [68] L. Madler, W. J. Stark, S. E. Pratsinis. *J Appl. Phys.* 2002, 92, 6537
- [69] C. Liewhiran, S. Phanichphant. *Sensors.* 2007, 7, 185
- [70] C. Liewhiran, A. Camenzind, A. Teleki, et al. *IEEE Trans. Nanotechnol.* 2007, Jan, 672
- [71] J. G. Lu, Z. Z. Ye, Y. Z. Zhang, et al. *Appl. Phys. Lett.* 2006, 89, 023122
- [72] J. G. Lu, Z. Z. Ye, Y. Z. Zhang, et al. *Appl. Phys. Lett.* 2006, 88, 063110
- [73] Y. S. Chang, Y. H. Chang, I. G. Chen, et al. *J Crystal Growth.* 2002, 243, 319
- [74] T. A. Kuriakose, S. N. Kalkura, M. Palanichamy, et al. *J Crystal Growth.* 2004, 263, 517
- [75] G. M. Wu, J. Wang, J. Shen, et al. *Materials Research Bulletin.* 2001, 36, 2127
- [76] X. Wang, Y. D. Li. *J. Am. Chem. Soc.* 2002, 124, 2880
- [77] M. Mo, J. H. Zeng, X. M. Liu, et al. *Adv. Mater.* 2002, 14, 1658
- [78] E. Hosono, S. Fujihara, K. Kakiuchi, et al. *J Am. Chem. Soc.* 2004, 126, 7790
- [79] J. M. Wang, L. Gao. *Solid State Commun.* 2004, 132, 269
- [80] B. Liu, H. C. Zeng. *J Am. Chem. Soc.* 2003, 125, 4430
- [81] Y. Sun, D. J. Riley, M. N. R. Ashfold. *J Phys. Chem. B.* 2006, 110, 15186
- [82] J. B. Liang, J. W. Liu, Q. Xie, et al. *J Phys. Chem. B.* 2005, 109, 9463
- [83] J. C. Ge, B. Tang, L. H. Zhou, et al. *Nanotechnology.* 2006, 17, 1316
- [84] M. Stefanescu, O. Stefanescu, M. Stoia, et al. *J Therm. Anal. Cal.* 2007, 88, 27
- [85] X. L. Li, X. X. Zhang, Z. R. Li, et al. *Solid State Commun.* 2006, 137, 581
- [86] J. R. A. Sietsma, J. D. Meeldijk, J. P. D. Breejen, et al. *Angew. Chem. Int. Ed.* 2007, 46, 4547
- [87] S. Maensiri, P. Laokul, V. Promarak. *J Crystal Growth.* 2006, 289, 102
- [88] H. Zhou, H. Alves, D. M. Hofmann, et al. *Appl. Phys. Lett.* 2002, 80, 210
- [89] H. Zhou, H. Alves, D. M. Hofmann, et al. *Phys. Stat. Sol.* 2002, 229, 825
- [90] J. P. Sylvestre, S. Poulin, A. V. Kabashin, et al. *J Phys. Chem. B.* 2004, 108, 16864
- [91] P. S. Liu, W. P. Cai, H. B. Zeng. *J Phys. Chem. C.* 2008, 112, 3261
- [92] K. V. Anikin, N.N. Melnik, A. V. Simakin, et al. *Chem. Phys. Lett.* 2002, 366, 357
- [93] J. L. Zhao, X. M. Li, J. M. Bian, et al. *J Crystal Growth.* 2005, 276, 507
- [94] D. H. A. Blank, H. Hilgenkamp, A. Brinkman, et al. *Appl. Phys. Lett.* 2001, 79, 394
- [95] A. V. Simakin, V. V. Voronov, N. A. Kirichenko, et al. *Appl. Phys. A.* 2004, 79, 1127
- [96] G. A. Shafeev, E. Freksz, F. B. Verduraz. *Appl. Phys. A.* 2004, 78, 307
- [97] J. Zhang, C. Q. Lan. *Materials Letters.* 2008, 62, 1521
- [98] C. H. Liang, Y. Shimizu, T. Sasaki, et al. *J Mater. Res.* 2004, 19, 1551
- [99] J. K. Muth, R. M. Kolbas, A. K. Sharma, et al. *J Appl. Phys.* 1999, 85, 7884
- [100] K. Y. Yun, M. Noda, M. Okuyama. *Appl. Phys. Lett.* 2003, 83, 3981

- [101] J. D. Ye, S. L. Gu, S. M. Zhu, et al. *J Crystal Growth*. 2002, 243, 151
- [102] P. A. Williams, J. L. Roberts, C. Jones, et al. *Chem. Vap. Deposition*. 2002, 8, 163
- [103] F. Hamelmann, G. Haindl, J. Schmalhorst, et al. *Thin Solid Films*. 2000, 358, 90
- [104] M. C. Jeong, B. Y. Oh, W. Lee, et al. *J Crystal Growth*. 2004, 268, 149
- [105] S.K.Lee, H. J. Choi, P. Pauzauskie, et al. *Phys. Stat. Sol.* 2004, 241, 2775
- [106] T. Minemoto, T. Negami, S. Nishiwaki, et al. *Thin Solid Films*. 2000, 372, 173
- [107] S. H. Jeong, B. S. Kim, B. T. Lee. *Appl. Phys. Lett.* 2003, 82, 2625
- [108] K. Zhang, F.R. Zhu, C. H. A. Huan, et al. *Thin Solid Films*. 2000, 376, 255
- [109] K. W. Kim, N. Koguchi, Y. W. Ok, et al. *Appl. Phys. Lett.* 2004, 84, 3810
- [110] A. Teleki, S. E. Pratsinis, K. Kalyanasundaram, et al. *Sens. Actuators B*. 2006, 119, 683
- [111] R. Mueller, R. Jossen, H. K. Kammler, et al. *AIChE J* 2004, 50, 3085
- [112] A. Killian, T. F. Morse. *Aerosol Sci. Technol.* 2001, 34, 227
- [113] R. Mueller, L. Madler, S. E. Pratsinis. *Chemical Engineering Science*. 2003, 58, 1969
- [114] T. Sahn, L. Madler, A. Gurlo, et al. *Sens. Actuators B*. 2004, 98, 148
- [115] R. Jissen, S. E. Pratsinis, W. J. Stark, et al. *J Am. Ceram. Soc.* 2005, 88, 1388
- [116] L. Madler, W.J. Stark, S. E. Pratsinis. *J Mater. Res.* 2002, 17, 1356
- [117] T. Tani, K. Takatori, S. E. Pratsinis. *J Am. Ceram. Soc.* 2004, 87, 365
- [118] S. Kim, J. J. Gislason, R. W. Morton, et al. *Chem. Mater.* 2004, 16, 2336
- [119] H. Schulz, W. J. Stark, M. Maciejewski, et al. *J Mater. Chem.* 2003, 13, 2979
- [120] J. Zhang, F. H. Jiang, L. D. Zhang. *J Phys. Chem. B*. 2004, 108, 7002
- [121] J. Y. Lee, D. S. Kim, J. Park. *Chem. Mater.* 2007, 19, 4663
- [122] C.X. Xu, X. W. Sun, Z. L. Dong, et al. *J Crystal Growth*. 2004, 270, 498
- [123] T. Gao, T. H. Wang. *J Crystal Growth*. 2006, 290, 660
- [124] D. W. Zeng, B. L. Zhu, C.S. Xie, et al. *Materials Science and Engineering A*. 2004, 366, 332
- [125] M. H. Huang, Y. Y. Wu, H. Feick, et al. *Adv. Mater.* 2001, 13, 113
- [126] X. H. Zhang, S. J. Chua, A. M. Yong. et al. *Appl. Phys. Lett.* 2007, 90, 013107
- [127] C. Li, G. J. Fang, J. Li, et al. *J Phys. Chem. C*. 2008, 112, 990
- [128] H. J. Fan, B. Fuhrmann, R. Scholz. *Nanotechnology*. 2006, 17, S231
- [129] S. J. Pearton, D. P. Norton, K. Ip, Y.W. Heo, T. Steiner, *Superlattices Microstruct.* 2003, 34, 3
- [130] M. L. Kahn, M. Monge, E. Snoeck, A. Maisonnat, B. Chaudret, *Small* 2005, 1, 221-224.
- [131] C. Pages, Y. Coppel, M. L. Kahn, A. Maisonnat, B. Chaudret, *Chemphyschem* 2009. 10. 2234.
- [132] K. Soullantica, A. Maisonnat, M.-C. Fromen, M.-J. Casanove, B. Chaudret, *Angew. Chem. Int. Ed.* 2003, 42, 1945.
- [133] F. Dumestre, B. Chaudret, C. Amiens, P. Renaud, P. Fejes, *Science* 2004, 303, 821.
- [134] L. Chen, J. Xu, J. D. Holmes, M. A. Morris, *J. Phys. Chem. C* 2010, 114, 2003.
- [135] Wang, L. J., Giles, N. C. *J Appl. Phys.* 2003, 94, 973.
- [136] Lin, K. F.; Cheng, H. M.; Hsu, H. C.; Lin, L. J.; Hsieh, W. F. *Chem. Phys. Lett.* 2005, 409, 208.
- [137] Zeghbrock, B. V. *Principles of Semiconductor Devices*, 2004.
- [138] Chanana, R. K.; Donald, K. M.; Ventra, M. D.; Pantelides, S. T.; Feldman, L. C.; Chung, G. Y.; Tin, C. C.; Williams, J. R.; Weller, R. A. *Appl. Phys. Lett.* 2000, 77, 2560.
- [139] Sze, S. M. *Physics of Semiconductor Devices*, 1981.
- [140] Fan, Z.; Lu, J. G. *J. Nanosci. Nanotechnol.* 2005, 5, 1561.
- [141] C. Y. Lee, Y. Y. Hui, W. F. Su. C. F. Lin, *Appl. Phys. Lett.* 2008, 92, 261107.

- [142] S. A. Maier, P. G. Kik, H. A. Atwater, S. Meltzer, E. Harel, B. E. Koel, A. A. G. Requicha, *Nature Mater.* 2003, 2, 229.
- [143] W. Nomura, M. Ohtsu, and T. Yatsui, *Appl. Phys. Lett.* 2005, 86, 181108.
- [144] T. Yatsui, Y. Ryu, T. Morishima, W. Nomura, T. Kawazoe, T. Yonezawa, M. Washizu, H. Fujita, M. Ohtsu, *Appl. Phys. Lett.* 2010, 96, 133106.
- [145] H. Oana, M. Ueda, and M. Washizu, *Biochem. Biophys. Res. Commun.* 1999, 265, 140.
- [146] T. Yatsui, H. Jeong, and M. Ohtsu, *Appl. Phys. B: Lasers Opt.* 2008, 93, 199.
- [147] M. Tammer, L. Horsburgh, A. P. Monkman, W. Brown, H. Burrows, *Adv. Funct. Mater.* 2002, 12, 447.
- [148] M. Campoy-Quiles, Y. Ishii, H. Sakai, H. Murata, *Appl. Phys. Lett.* 2008, 92, 213305.
- [149] B. Gil, A. V. Kavokin, *Appl. Phys. Lett.* 2002, 81, 748.

IntechOpen



Optoelectronic Devices and Properties

Edited by Prof. Oleg Sergiyenko

ISBN 978-953-307-204-3

Hard cover, 660 pages

Publisher InTech

Published online 19, April, 2011

Published in print edition April, 2011

Optoelectronic devices impact many areas of society, from simple household appliances and multimedia systems to communications, computing, spatial scanning, optical monitoring, 3D measurements and medical instruments. This is the most complete book about optoelectromechanic systems and semiconductor optoelectronic devices; it provides an accessible, well-organized overview of optoelectronic devices and properties that emphasizes basic principles.

How to reference

In order to correctly reference this scholarly work, feel free to copy and paste the following:

Ting Mei and Yong Hu (2011). Synthesis, Self-assembly and Optoelectronic Properties of Monodisperse ZnO Quantum Dots, Optoelectronic Devices and Properties, Prof. Oleg Sergiyenko (Ed.), ISBN: 978-953-307-204-3, InTech, Available from: <http://www.intechopen.com/books/optoelectronic-devices-and-properties/synthesis-self-assembly-and-optoelectronic-properties-of-monodisperse-zno-quantum-dots>

INTECH
open science | open minds

InTech Europe

University Campus STeP Ri
Slavka Krautzeka 83/A
51000 Rijeka, Croatia
Phone: +385 (51) 770 447
Fax: +385 (51) 686 166
www.intechopen.com

InTech China

Unit 405, Office Block, Hotel Equatorial Shanghai
No.65, Yan An Road (West), Shanghai, 200040, China
中国上海市延安西路65号上海国际贵都大饭店办公楼405单元
Phone: +86-21-62489820
Fax: +86-21-62489821

© 2011 The Author(s). Licensee IntechOpen. This chapter is distributed under the terms of the [Creative Commons Attribution-NonCommercial-ShareAlike-3.0 License](#), which permits use, distribution and reproduction for non-commercial purposes, provided the original is properly cited and derivative works building on this content are distributed under the same license.

IntechOpen

IntechOpen